Monte Carlo Simulation of Electron Transport in Quantum Cascade Lasers

O. Baumgartner, Z. Stanojevic, H. Kosina

1 Sep. 2011

Institute for Microelectronics
Gußhausstraße 27-29/E360
A-1040 Vienna, Austria

Outline

Introduction Quantum Cascade Lasers

Pauli master equation

Basis functions

Results

Conclusions

Quantum Cascade Laser

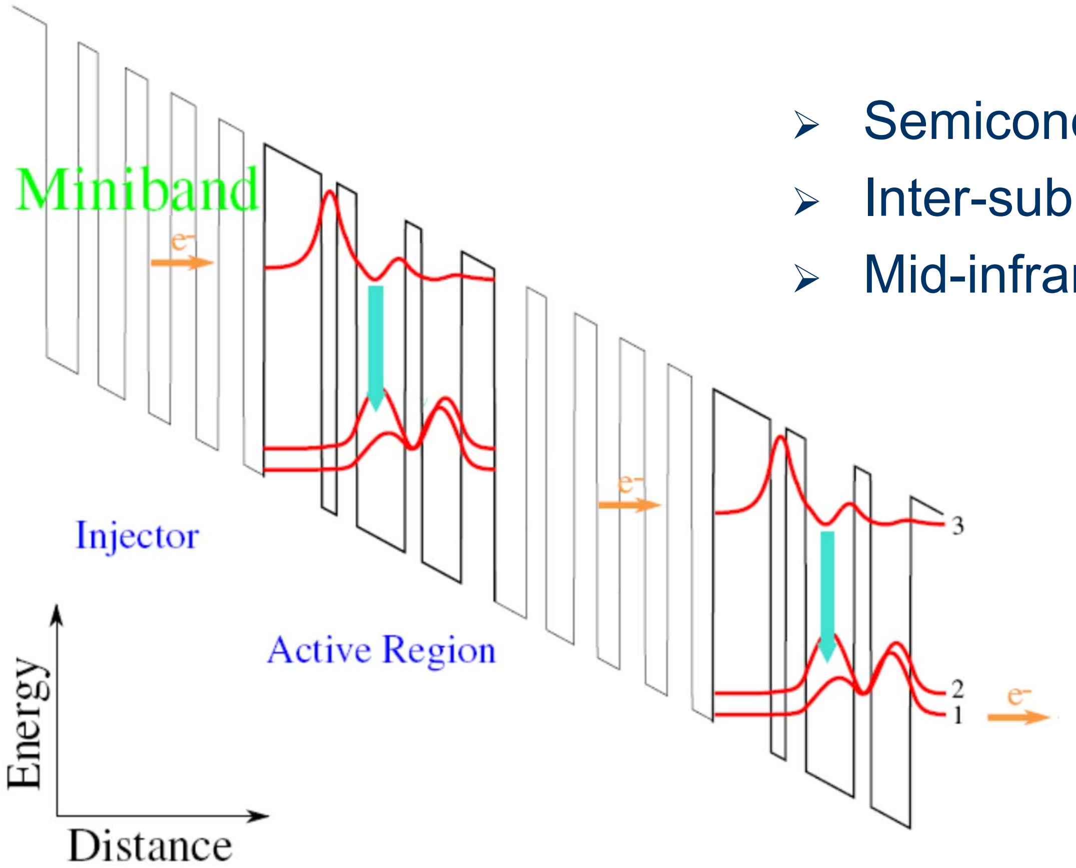

- Semiconductor heterostructure
- Inter-subband transitions
- Mid-infrared to THz emission

R. Kazarinov, R. Suris, Sov.Phys. Sem **5**, 1971

J. Faist, F. Capasso et al., Science **264**, 1994

Quantum Cascade Laser: Applications

Spectroscopic applications

- Medical diagnostics
- Sensing of environmental gases
- Sensing of pollutants in the atmosphere
- Sensing of heavy molecules, e.g. in explosives, toxic chemicals

Automotive

- Vehicular cruise control
- Collision avoidance radar
- Combustion control

Industrial process control

Transport Equation

Coherent Quantum Transport

Weakly coupled quantum wells (right figure)

- Two energy levels aligned (resonance)
- Tunneling of localized wave packet between left and right well
- **Transport is limited by coherent tunneling** ($\Omega \ll \omega_{21}$)

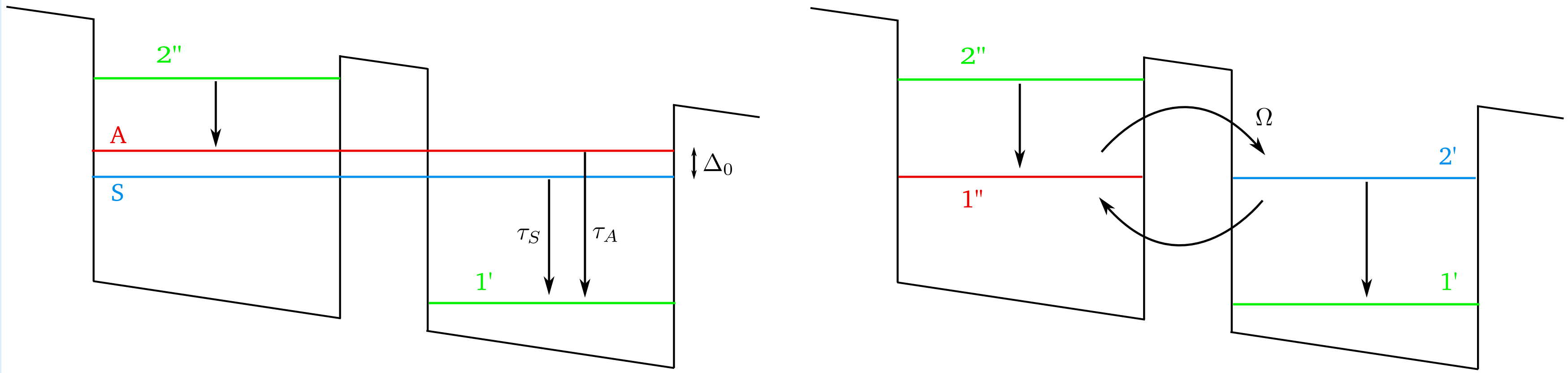

Semiclassical Picture   Coherent Picture

Incoherent Quantum Transport

Strongly coupled quantum wells (left figure)

- Two states in resonance (anti-crossing)
- Extended states form: symmetric (S) and antisymmetric (A)
- **Transport is limited by incoherent scattering** ($1/\tau_{S}$, $1/\tau_{A} \ll \Omega$)

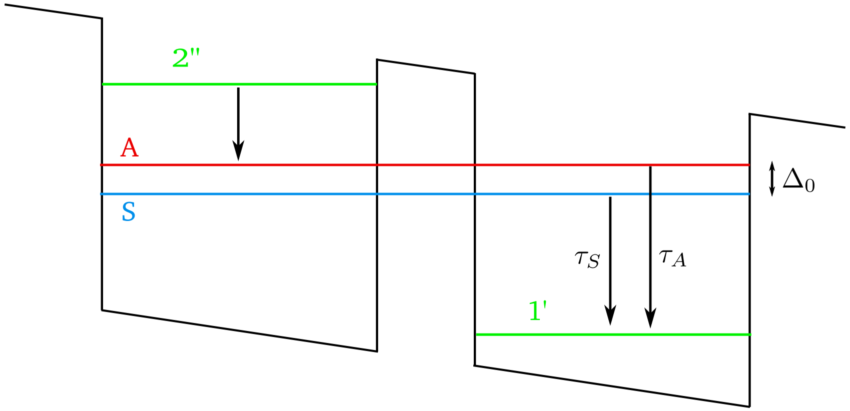

Semiclassical Picture

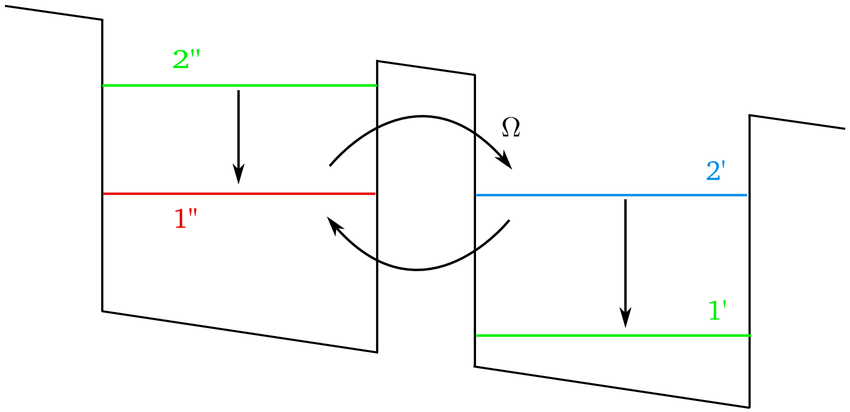

Coherent Picture

Pauli Master Equation (PME)

The PME is obtained as a long-time limit from the Liouville-von Neumann equation (Markov approximation)

- The PME is a semi-classical, Boltzmann-like kinetic equation

$$\frac{\mathrm{d}f_{\mathbf{k},n}(t)}{\mathrm{d}t} = \sum_{\mathbf{k}',m} \left\{ S_m^n(\mathbf{k}',\mathbf{k})\, f_{\mathbf{k}',m}(t) - S_n^m(\mathbf{k},\mathbf{k}')\, f_{\mathbf{k},n}(t) \right\}$$

$f_{\mathbf{k},n}(t)$ … subband distribution functions (positive)

$\mathbf{k}$ … in-plane wave vector

n … subband index

The PME is solved by a Monte Carlo method

Pauli Master Equation: Assumptions

When the electron de-phasing length in the contacts λ_φ is larger than the length of the device L, the electrons are considered to be ”larger” than the device.

Following Van Hove’s observation, the time needed to build the off-diagonal elements of ρ is much longer than the relaxation and transit times
$\Rightarrow$ Master equation considering only diagonal elements ρ_{ii} is sufficient for $L < \lambda_\varphi$

Applicable to (quasi) stationary systems only (current conservation)

L. Van Hove, Physica XXI 1955

Boundary Conditions for the PME

N-terminal device

- Exchange of electrons with external reservoirs (contacts)
- Relaxation-time-like term is added

$$\left.\frac{d}{dt} f_{\mathbf{k}\alpha}\right|_{\mathrm{res}} = \gamma_{\mathbf{k}\alpha}(f^0_{\mathbf{k}\alpha} - f_{\mathbf{k}\alpha})$$

Quantum cascade laser

- Apply periodic BCs
- Electron is re-injected into the central stage with energy difference

$$\Delta_{\lambda\lambda'} = eFL(\delta_{\lambda',\lambda+1} - \delta_{\lambda',\lambda-1})$$

- Current calculation: Count inter-stage scattering events

Basis Functions

Band Structure Model

QCLs are made of III-V compound semiconductors

- Direct band gap → band structure around Γ-point is relevant
- Band non-parabolicity is important → use $\mathbf{k}\cdot\mathbf{p}$ method
- Size quantization in superlattice: $p_z = \hbar k_z = -i\hbar\frac{\partial}{\partial z}$

Example: Six-band Hamiltonian for the valence band

$$\mathbf{H}_{6\times 6} = \mathcal{E}_\mathrm{v}\mathbf{I}_{6\times 6} + \begin{bmatrix} \mathbf{S}+\mathbf{D} & \mathbf{0}_{3\times 3} \\ \mathbf{0}_{3\times 3} & \mathbf{S}+\mathbf{D} \end{bmatrix} + \mathbf{H}_{\mathbf{so},6\times 6}$$

$$\mathbf{S}=\begin{bmatrix} Lk_\mathrm{x}^2+M(k_\mathrm{y}^2+k_\mathrm{z}^2) & Nk_\mathrm{x}k_\mathrm{y} & Nk_\mathrm{x}k_\mathrm{z} \\ Nk_\mathrm{x}k_\mathrm{y} & Lk_\mathrm{y}^2+M(k_\mathrm{x}^2+k_\mathrm{z}^2) & Nk_\mathrm{y}k_\mathrm{z} \\ Nk_\mathrm{x}k_\mathrm{z} & Nk_\mathrm{y}k_\mathrm{z} & Lk_\mathrm{z}^2+M(k_\mathrm{x}^2+k_\mathrm{y}^2) \end{bmatrix}$$

Band Structure Model

Example: Six-band Hamiltonian for the valence band

- Strain effects

$$\mathbf{D}=\begin{bmatrix} l\varepsilon_{\mathrm{xx}}+m(\varepsilon_{\mathrm{yy}}+\varepsilon_{\mathrm{zz}}) & n\varepsilon_{\mathrm{xy}} & n\varepsilon_{\mathrm{xz}} \\ n\varepsilon_{\mathrm{xy}} & l\varepsilon_{\mathrm{yy}}+m(\varepsilon_{\mathrm{xx}}+\varepsilon_{\mathrm{zz}}) & n\varepsilon_{\mathrm{yz}} \\ n\varepsilon_{\mathrm{xz}} & n\varepsilon_{\mathrm{yz}} & l\varepsilon_{\mathrm{zz}}+m(\varepsilon_{\mathrm{xx}}+\varepsilon_{\mathrm{yy}}) \end{bmatrix}$$

- Spin orbit interaction

$$\mathbf{H}_{\mathbf{so},6\times6} = -\frac{\mathcal{E}_{\mathrm{so}}}{3}\begin{bmatrix} 0 & \mathrm{i} & 0 & 0 & 0 & -1 \\ -\mathrm{i} & 0 & 0 & 0 & 0 & \mathrm{i} \\ 0 & 0 & 0 & 1 & -\mathrm{i} & 0 \\ 0 & 0 & 1 & 0 & -\mathrm{i} & 0 \\ 0 & 0 & \mathrm{i} & \mathrm{i} & 0 & 0 \\ -1 & -\mathrm{i} & 0 & 0 & 0 & 0 \end{bmatrix}$$

T. Manku, A. Nahtan, J.Appl.Phys **73** (1993)

BCs for the Schrödinger Equation

Closed boundaries

- Dirichlet BC
- Discrete energy levels
- No current

Open boundaries

- Plane wave BC
- Continuous energy spectrum
- **No current**

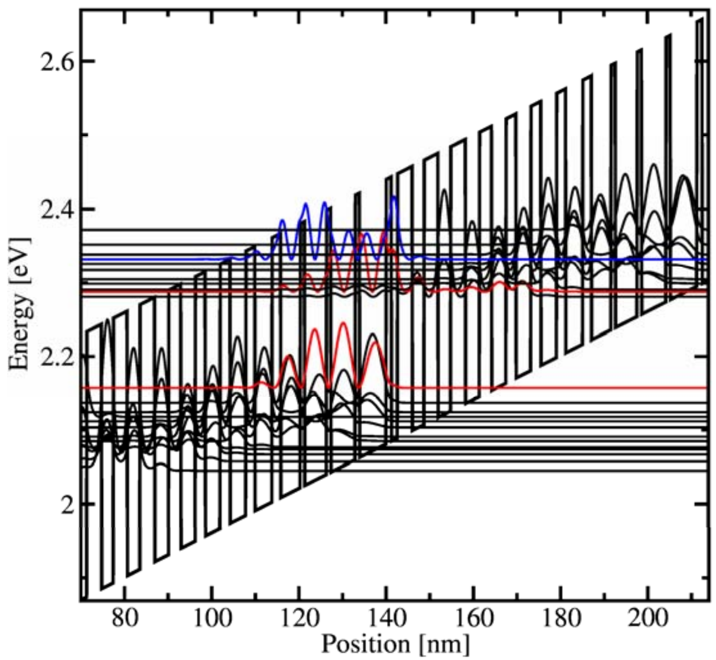

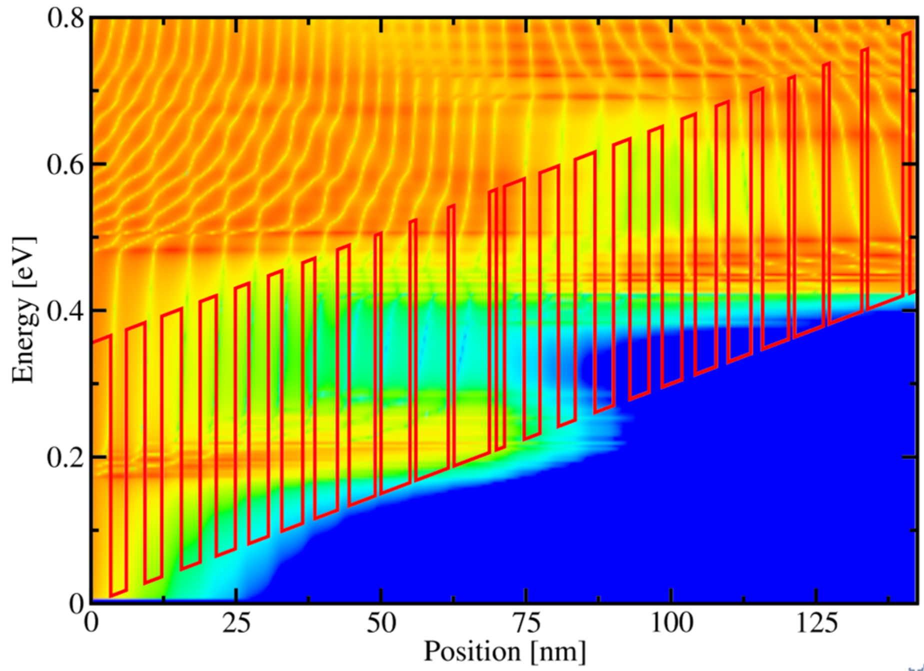

Inchoherent scattering is needed to allow current flow!

Perfectly Matched Layer BC

- Widely used in electromagnetic simulations
- Used for band structure calculation of open systems (Odermatt 2005)

- Based on complex coordinate stretching
  $\tilde{x} = \int_0^x s_x(\tau)\,\mathrm{d}\tau$
- Evaluation of ∇ yields
  $\frac{\partial}{\partial \tilde{x}} = \frac{1}{s_x(x)} \frac{\partial}{\partial x}$

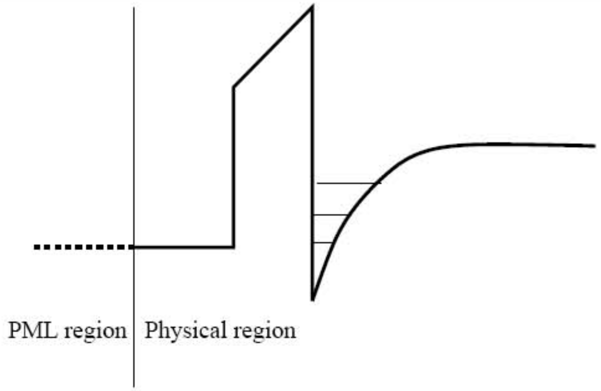

Allows to create absorbing layers

- An absorbing layer is added to prevent reflections at the boundary
- The system remains quasi-open although Dirichlet boundary conditions are applied
- The Hamiltonian becomes non-Hermitian and admits complex eigenvalues $\mathcal{E} = \mathcal{E}_r + \imath \mathcal{E}_i$

BCs for the Schrödinger Equation

Dirichlet BC (closed system)

- Bound states

Perfectly matched layer BC (open system)

- Quasi-bound states, finite life times

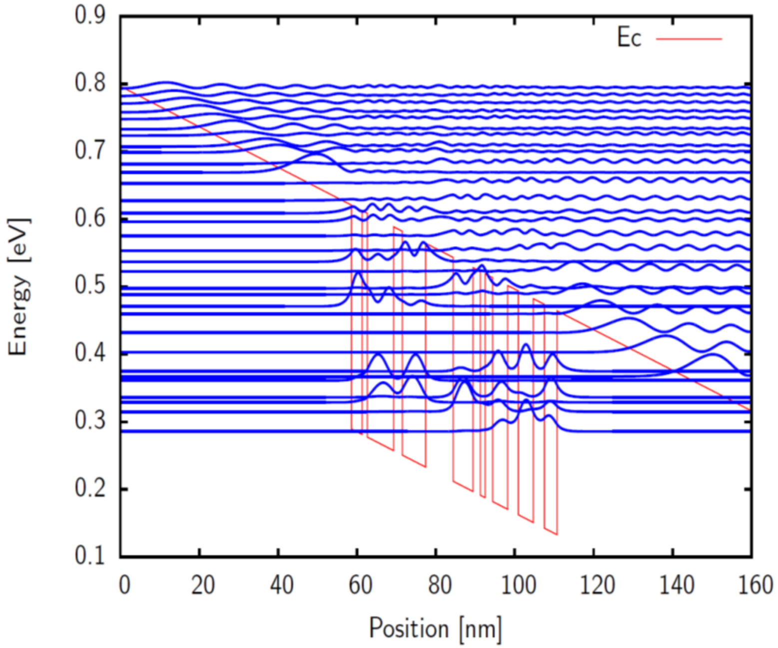

Dirichlet BC

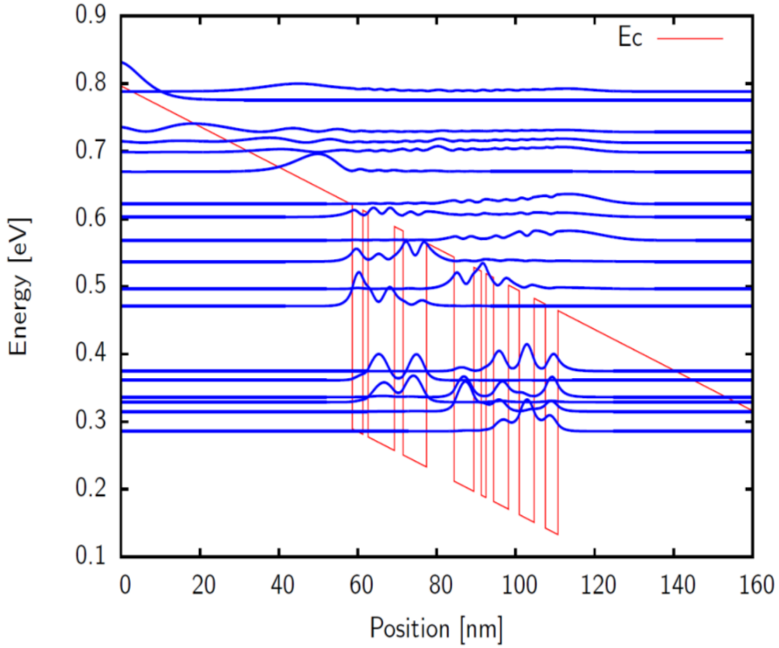

Perfectly matched layer BC

Selection of Field-periodic States

Calculate the cross-correlation functions of all wave functions

- If a c.c.f. has a maximum at x = L, accept the two wave functions
- All spurious states due to artificial boundaries are removed

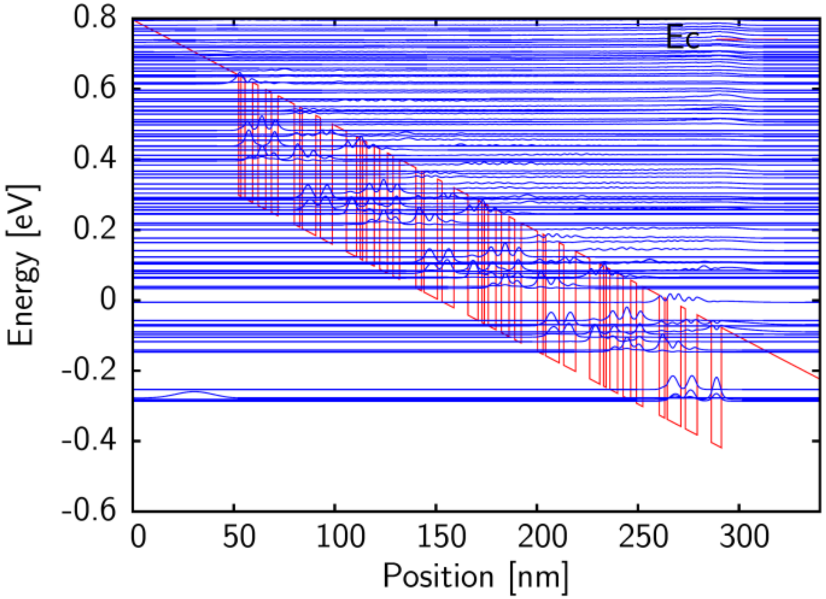

Field-periodic and spurious states

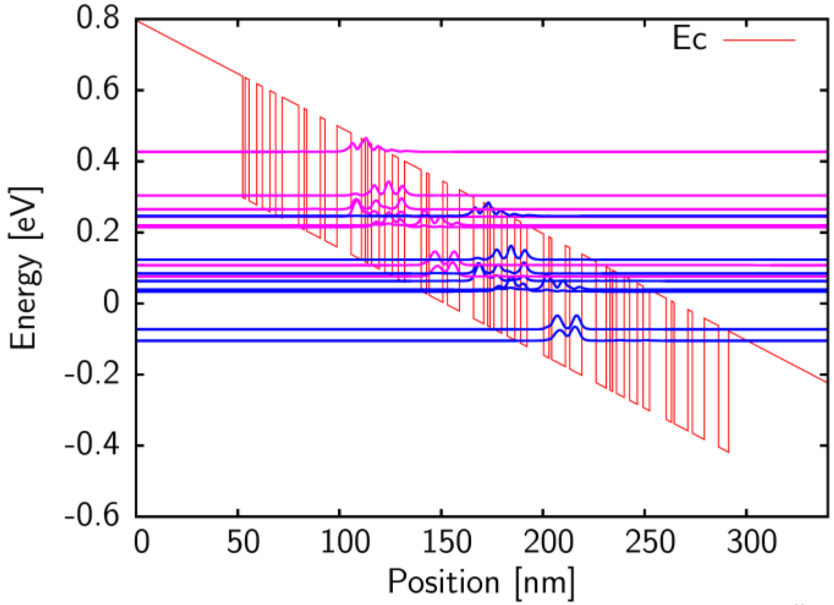

Field-periodic states only

Electron Scattering Processes

Electron Scattering

Transition rate from state $|\mathbf{k}, n\rangle$ to state $|\mathbf{k}', m\rangle$ is given by Fermi´s Golden Rule

$$S_n^m(\mathbf{k}, \mathbf{k}') = \frac{2\pi}{\hbar} \left|\langle \mathbf{k}', m | H_{\mathrm{int}} | \mathbf{k}, n\rangle\right|^2 \delta\left(\mathcal{E}(\mathbf{k}') - \mathcal{E}(\mathbf{k}) \mp \hbar\omega\right)$$

Scattering processes due to

- Acoustic and optical deformation potential interaction
- Inter-valley phonons
- Polar-optical (PO) phonons
- Interface roughness
- Alloy disorder
- (e-photon interaction, e-e interaction)

Electron Scattering by PO phonons

Fröhlich Hamiltonian: Matrix element is q-dependent

Total scattering rate

- Evaluation of the matrix element requires a numerical integration
- Integration over all final states

$$\Gamma_{mn}(\mathbf{k}_{\parallel}) = \frac{m^*}{\hbar^2}\frac{e^2\omega_{\mathrm{PO}}}{4\pi\varepsilon}\left(n_{\mathrm{PO}} + \tfrac{1}{2} \mp \tfrac{1}{2}\right)\int \frac{\left|\widehat{\rho}_{mn}(q_{\mathrm{z}})\right|^2}{\sqrt{(k_{\parallel}^2 + k_f^2 + q_{\mathrm{z}}^2)^2 - 4k_{\parallel}^2 k_f^2}}\mathrm{d}q_{\mathrm{z}}$$

$$\widehat{\rho}_{mn}(q_{\mathrm{z}}) = \mathcal{F}\{\rho_{mn}(z)\}$$

$$\rho_{mn}(z) = \psi_m^*(z)\psi_n(z)$$

Reordering of the integrations gives speed up of 3 to 4 orders

Data Structures

The scattering rates are precalculated and stored in a look-up table

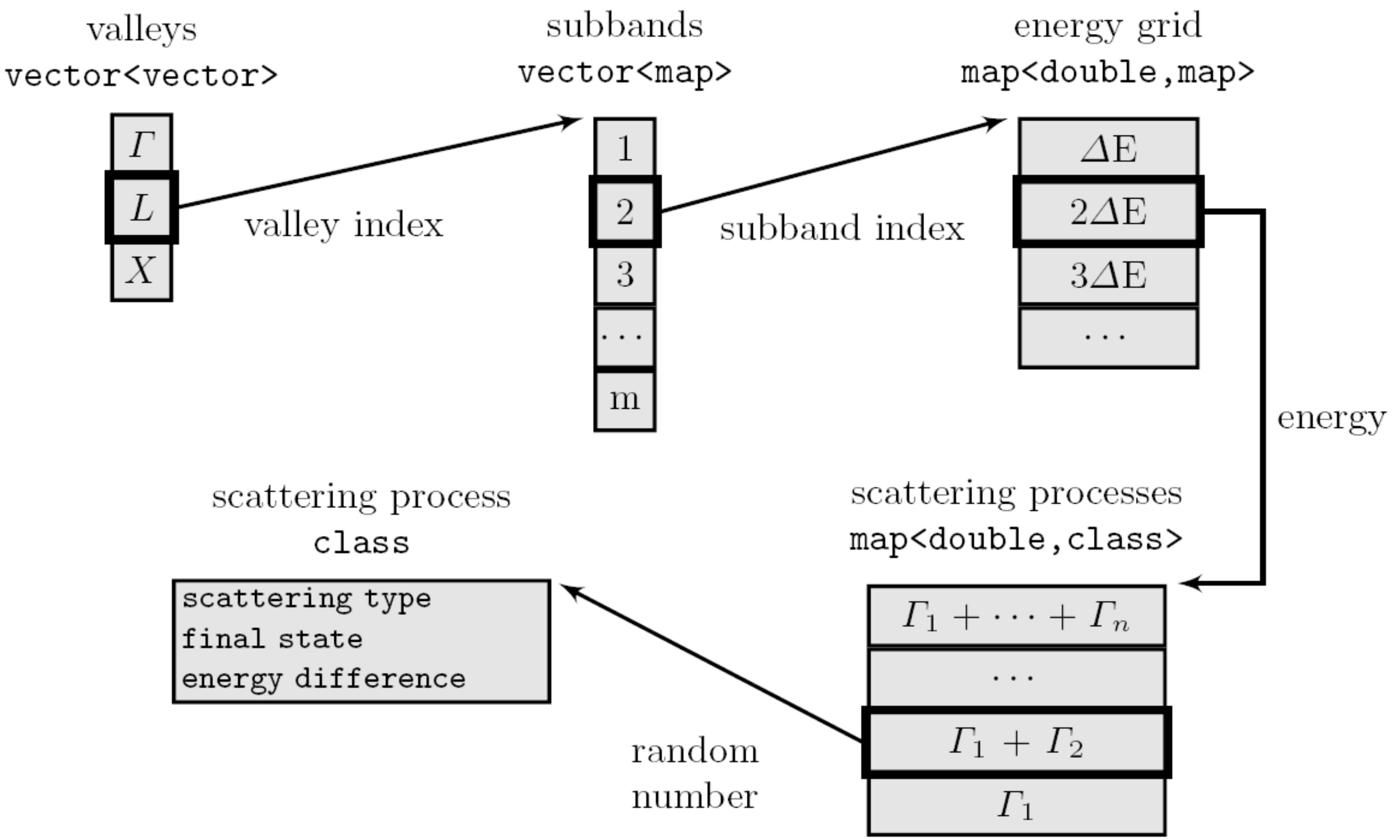

Results

Mid Infrared QCL

Material system:

$In_{0.53}Ga_{0.47}As/GaAs_{0.51}Sb_{0.49}$

Layer sequence in nm:

8.1, 2.7, **1.3**, 6.7, **2.2**, 5.9, **7.0**, 5.0, **1.9**, 1.2, **1.9**, <u>3.8</u>, **2.7**, <u>3.8</u>, **2.8**, 3.2.

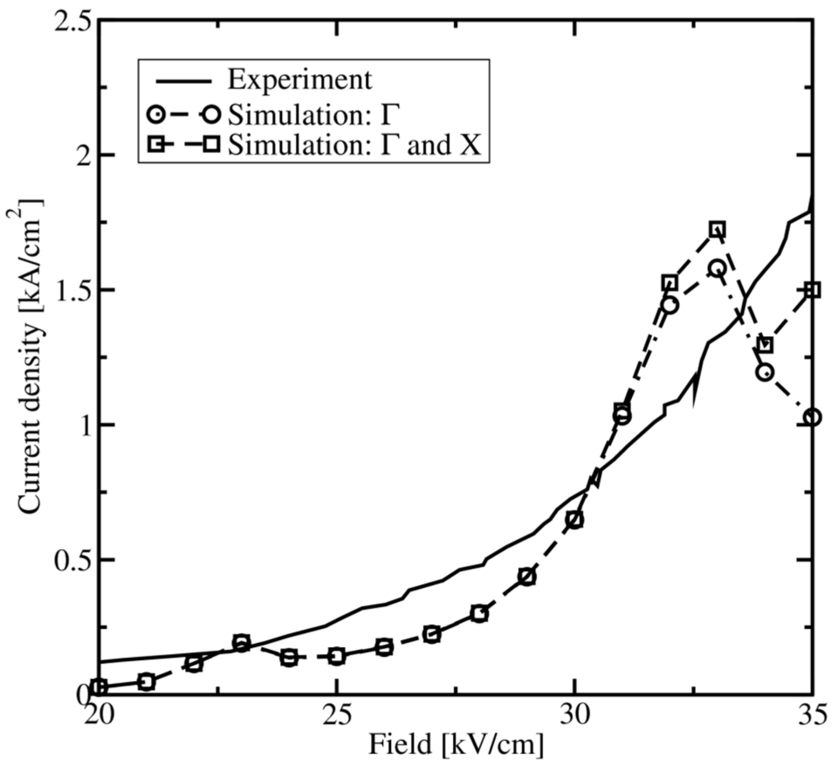

Nobile et al., El. Lett. (2008)

Mid Infrared QCL

Solve Pauli Master equation for electronic transport including all relevant scattering processes

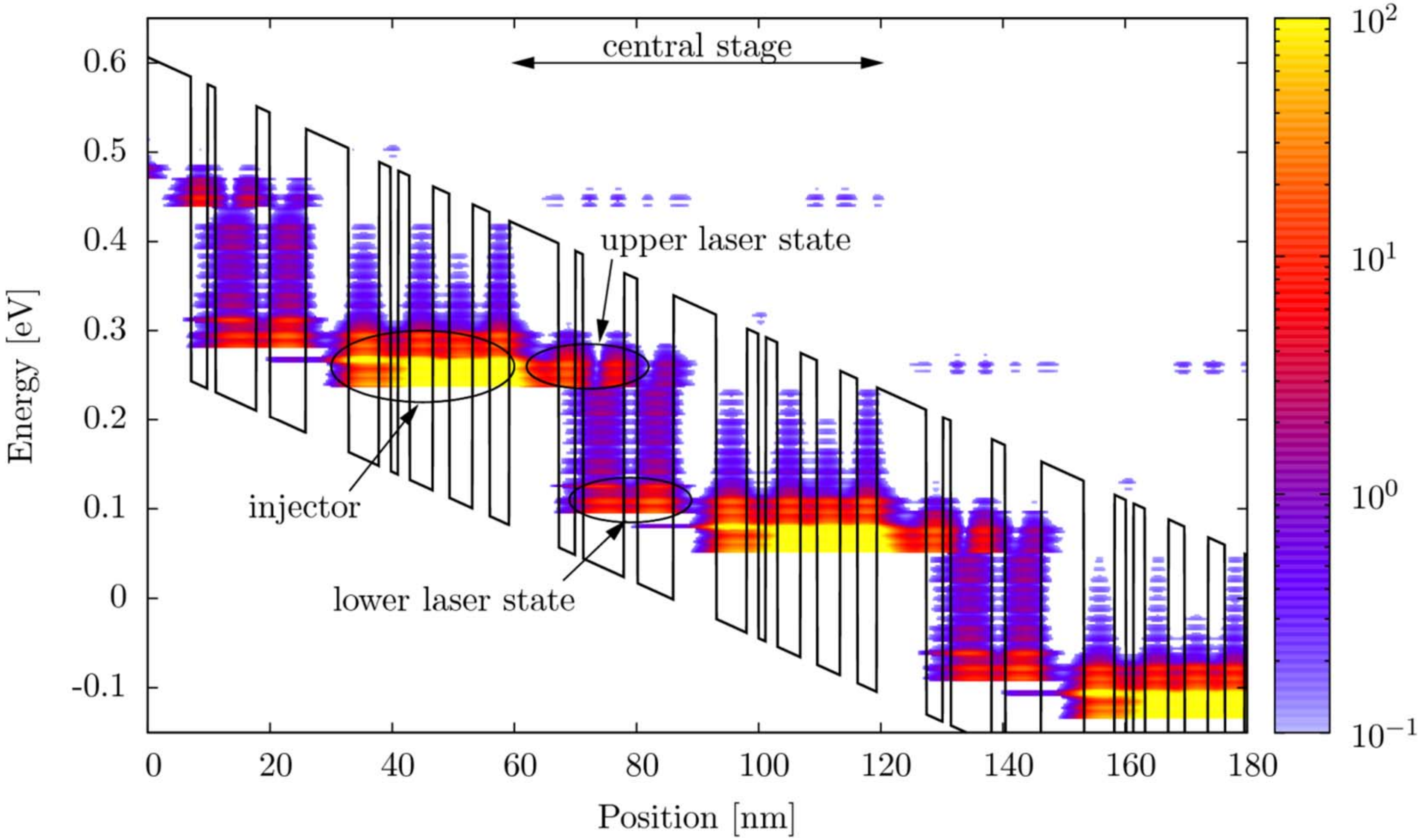

Electron density spectrum

THz Quantum Cascade Laser

GaAs/$Al_{0.15}Ga_{0.85}As$ material system

Layer sequence in namometers: 9.2,**3**,15.5,**4.1**,6.6,**2.7**,8,**5.5**

E = 10 kV/cm, T = 70K

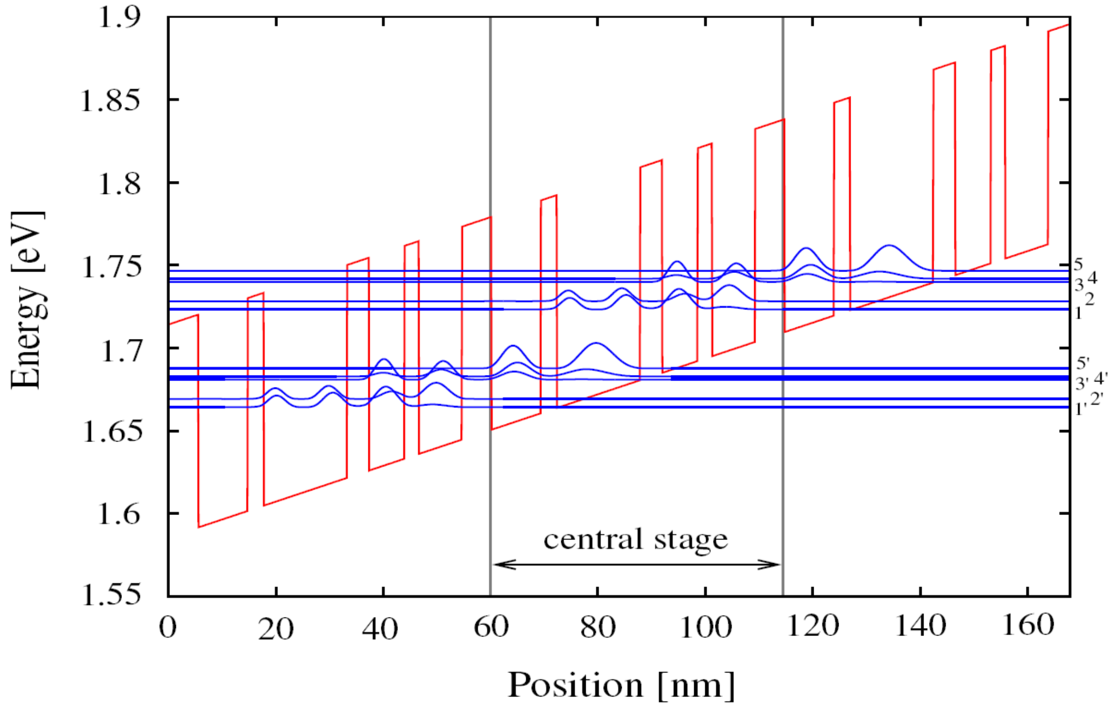

Band diagram and squared wave functions

THz Quantum Cascade Laser

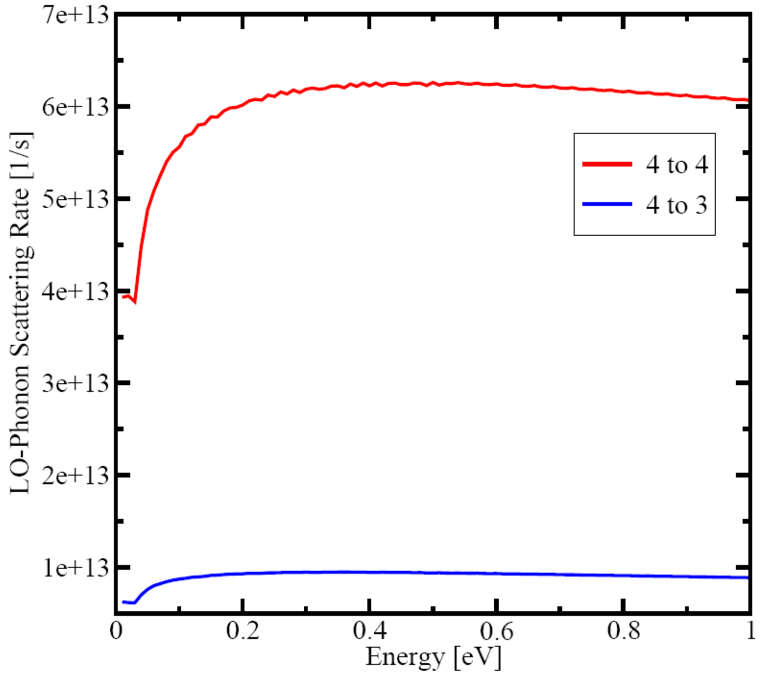

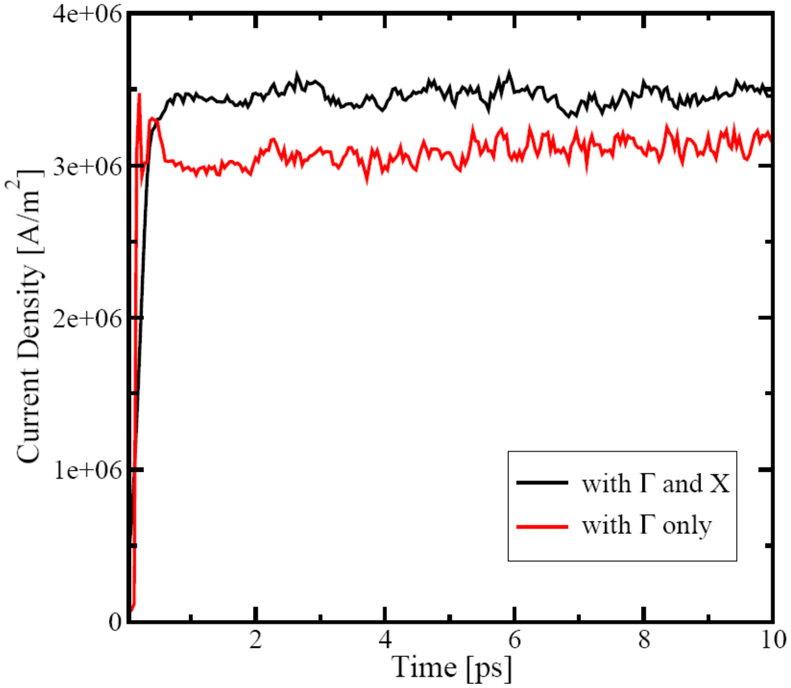

PO-phonon scattering rates 4 → 4 and 4 → 3 at E = 10 kV/cm and T = 70 K

Time evolution of the current (ensemble Monte Carlo method)

THz Quantum Cascade Laser

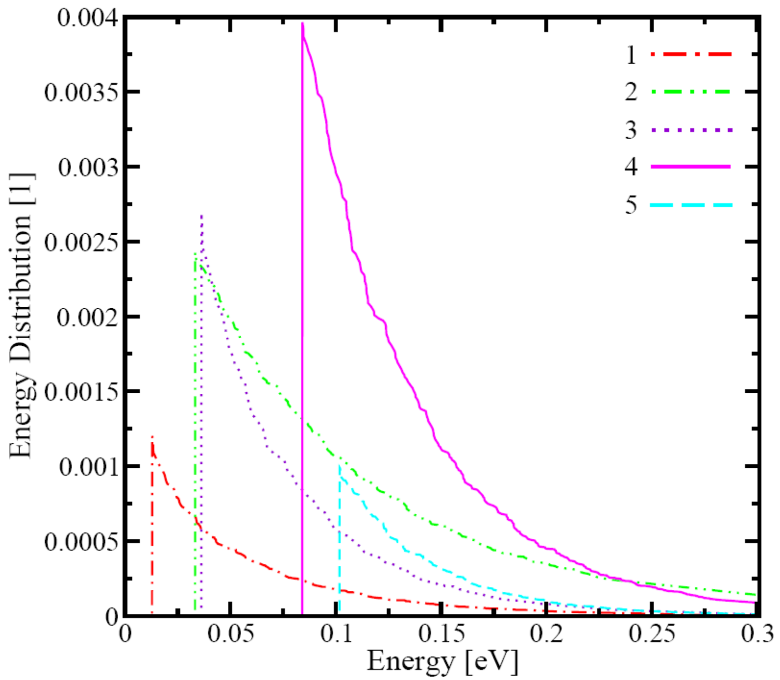

Energy distribution functions of the
Individual subbands

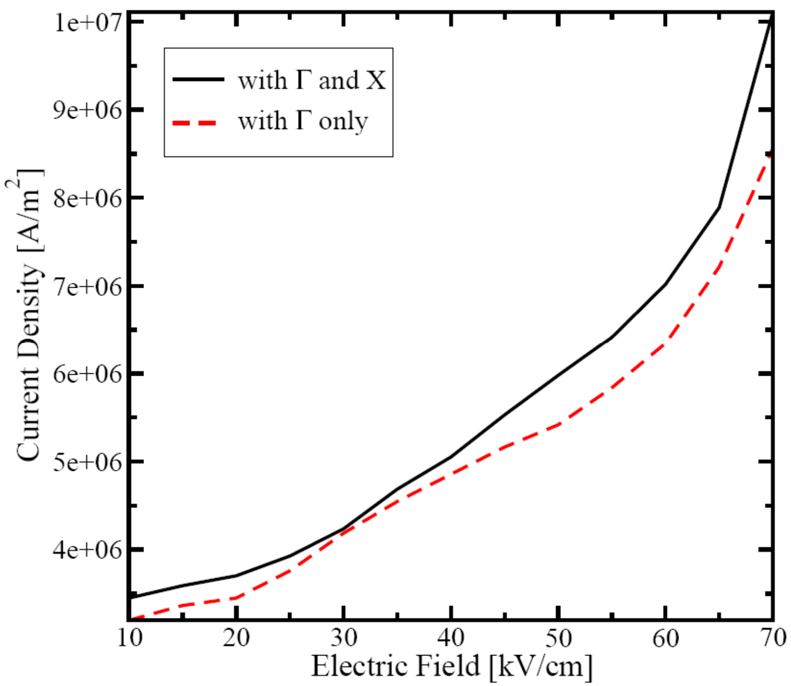

Current density with and without
X-valley transport

Conclusions

A semi-classical transport model can be orders of magnitude faster than a full quantum transport model (non-equilibrium Green's functions, full density matrix)

In many cases, structures of realistic complexity (geometry, physics) can only be modeled semi-classically

Applicability needs to be checked for every case

Some problems cannot be handled, e.g. ultrafast relaxation processes, coherent tunneling